Tunable coupling regimes of silicon microdisk resonators using MEMS actuators

Ming-Chang M. Lee

Institute of Photonics Technologies, National Tsing Hua University, 30055, Taiwan
mclee@ee.nthu.edu.tw

Ming C. Wu

Department of Electrical Engineering and Computer Sciences, University of California, Berkeley, CA 94720, USA
wu@eecs.berkeley.edu

Abstract: Tunable coupling regimes of a silicon microdisk resonator controlled by MEMS (microelectromechanical system) actuation are demonstrated for the first time. By varying the gap spacing between the waveguide and the disk, this microresonator can dynamically operate in either under-, ciritcal or over-coupling regime. The waveguide transmittance is suppressed by 30 dB in critical coupling, and the quality factor of the microdisk is measured to be as high as 10^5. Additionally, the microdisk presents tunable group delay from 27 ps to 65 ps, and tunable group velocity dispersion from 185 ps/nm to 1200 ps/nm. Waveguides, microdisks and actuators are all integrated on a silicon-on-insulator (SOI) substrate. This compact device exhibits the promise to construct resonator-based reconfigurable photonic integrated circuits.

©2006 Optical Society of America

OCIS codes: (130.3120) Integrated optics devices; (230.5750) Resonators.

References and links

1. B. E. Little, S. T. Chu, W. Pan, and Y. Kokubun, "Microring resonator arrays for VLSI photonics," IEEE Photonics Technol. Lett. **12**, 323-325 (2000).
2. C. K. Madsen, G. Lenz, A. J. Bruce, M. A. Cappuzzo, L. T. Gomez, T. N. Nielsen, L. E. Adams, and I. Brenner, "An all-pass filter dispersion compensator using planar waveguide ring resonators," presented at OFC/IOOC'99. Optical Fiber Communication Conference and the International Conference on Integrated Optics and Optical Fiber Communications (Cat. No.99CH36322). IEEE. Part vol.4, 1999, pp.99-101 vol.4. Piscataway, NJ, USA.
3. P. Rabiei, W. H. Steier, Z. Cheng, W. Chuan-guang, and H. J. Lee, "Polymer micro-ring modulator with 1 THz FSR," presented at Postdeadline Papers. Summaries of papers presented at the Conference on Lasers and Electro-Optics. Conference Edition (IEEE Cat. No.02CH37337). (Optical Society of America, Washington, D.C., 2002) Part vol.2, pp.CPDB8-1-CPDC2-3 vol.2..
4. K. Djordjev, C. Seung-June, C. Sang-Jun, and R. D. Dapkus, "Microdisk tunable resonant filters and switches," IEEE Photonics Technol. Lett. **14,** 828-30 (2002).
5. G. N. Nielson, D. Seneviratne, F. Lopez-Royo, P. T. Rakich, F. Giacometti, H. L. Tuller, and G. Barbastathis, "MEMS based wavelength selective optical switching for integrated photonic circuits," presented at Conference on Lasers and Electro-Optics (CLEO). IEEE. Part vol.1, 2004, pp.2 pp. vol.1. Piscataway, NJ, USA.
6. K. Djordjev, C. Seung-June, C. Sang-Jun, and P. D. Dapkus, "Vertically coupled InP microdisk switching devices with electroabsorptive active regions," IEEE IEEE Photonics Technol. Lett. **14,** 1115-17 (2002).
7. K. Djordjev, C. Seung-June, C. Sang-Jun, and P. D. Dapkus, "Gain trimming of the resonant characteristics in vertically coupled InP microdisk switches," Appl. Phys. Lett. **80,** 3467-3469 (2002).
8. W. M. J. Green, R. K. Lee, A. Yariv, and A. Scherer, "Control of optical waveguide-resonator coupling: applications to low-power optical modulation and switching," presented at 2003 IEEE LEOS Annual Meeting Conference Proceedings (IEEE Cat. No.03CH37460). IEEE. Part vol.1, 2003, pp.130-1 vol.1. Piscataway, NJ, USA.
9. M. Borselli, K. Srinivasan, P. E. Barclay, and O. Painter, "Rayleigh scattering, mode coupling, and optical loss in silicon microdisks," Appl. Phys. Lett. **85,** 3693-3695 (2004).
10. M. C. M. Lee and M. C. Wu, "MEMS-Actuated microdisk resonators with variable power coupling ratios," IEEE Photonics Technol. Lett. **17,** 1034-1036 (2005).

#68804 - $15.00 USD Received 8 March 2006; accepted 5 May 2006

11. S. D. Senturia, *Microsystem Design* (Kluwer Academic, 2001).
12. M. C. M. Lee, J. Yao, and M. C. Wu, "Silicon Profile Transformation and Sidewall Roughness Reduction Using Hydrogen Annealing," presented at 18th IEEE International Conference on Micro-Electro-Mechanical-Systems, Miami, 2005.
13. M. Matsuhara and A. Watanabe, "Coupling of curved transmission lines, and application to optical directional couplers," J. Opt. Soc. Am. **65,** 163-168 (1975).
14. B. E. Little, S. T. Chu, H. A. Haus, J. Foresi, and J. P. Laine, "Microring resonator channel dropping filters," J. Lightwave Technol. **15,** 998-1005 (1997).

1. Introduction

Integrated microdisk or microring resonators recently received a great deal of interest to realize on-chip wavelength-division-multiplexed (WDM) devices, such as add-drop multiplexers [1] and dispersion compensators [2]. Semiconductor microdisks are advantageous to reduce the device size due to the high index contrast, resulting in wide free-spectral-ranges and compactness. They are key building blocks to implement multiple functions in photonic integrated circuits (PICs). Adding tuning mechanisms to microresonators is further attractive for dynamic reconfigurable optical systems. Most of the tunable microresonators reported to date were demonstrated by manipulating either the resonant wavelength or the resonator loss. The former shifts the transmission spectrum while the latter varies the transmission intensity at resonant wavelengths. The resonant wavelengths are usually tuned by local heating [3] or electrical carrier injection [4]. On the other hand, the resonator loss can be adjusted by attaching a lossy material, such as a metal film, on the resonator [5], or by electroabsorption [6] and gain-trimming [7] in case of III-V semiconductors. However, the induced resonator loss, in most cases, also shifts the resonant wavelengths due to the Kramers-Kronig relation. It is difficult to separate these two correlated effects. The other tuning mechanism is varying the coupling between the waveguides and the resonator. A tunable MZI coupler [8] was reported to control the coupling in a ring resonator, but it is not suitable for small microresonators. Another approach is building a bulk mechanical setup to probe the semiconductor microresonator with optical fibers [9]. However, the refractive index of optical fiber is difficult to match with that of semiconductors and this technique is also challenging to be employed in integrated optical systems.

Directly varying the gap spacing between the integrated waveguide and microresonator is much efficient for tuning the coupling. For a silicon microdisk resonator, the coupling coefficient can be varied over many orders of magnitude just by controlling the gap spacing with a variation of 1 μm. Since MEMS can achieve high-resolution movement, it is ideal for moving the waveguides or the microdisks to control the gap spacing. Previously, a laterally coupled MEMS-actuated microdisk resonator was demonstrated to vary the power coupling ratio for the first time [10]. However, the device can only operate in the under-coupling regime due to a low intrinsic quality factor (Q). In this paper, a high-Q and vertically coupled microdisk resonator is exhibited with the capability of operating the device in all the under-coupling, critical coupling, and over-coupling regimes. Microresonators with tunable coupling regimes can realize a variety of applications such as dynamic add-drop filters and wavelength-selective optical switches. Meanwhile, in resonator-based optical circuits, the transmission phase is also affected by the waveguide-resonator coupling. Thus, the MEMS-actuated microdisk resonator can be a fundamental tunable element in silicon photonic integrated circuits.

2. Device schematic and fabrication

Figure 1 illustrates the schematic structure of the MEMS-actuated vertically-coupled Si microdisk. Two layers of single-crystalline silicon (0.25-μm thickness) are stacked on a silicon substrate. The microdisk (20-μm radius) and the MEMS electrodes are patterned on the bottom layer, while the waveguides (0.8-μm width) are fabricated on the top layer. These two layers are separated with a spacer of 1-μm-thick SiO_2. At the center of the device, the waveguides are released by removing the underlying SiO_2 and aligned to the microdisk edge

#68804 - $15.00 USD Received 8 March 2006; accepted 5 May 2006

to excite whispering gallery modes (WGMs). These suspended waveguides can be deformed by an electrostatic force as a voltage is applied on the bottom electrodes. Thus, the gap spacing between the waveguide and the microdisk decreases as a function of the applied voltage. To allow for a continuous variation of the gap spacing from 1 μm to near-contact without pull-in [11], comb-like electrostatic actuators are employed on both ends of the suspended waveguide, as shown in the cross-sectional views in Fig. 1.

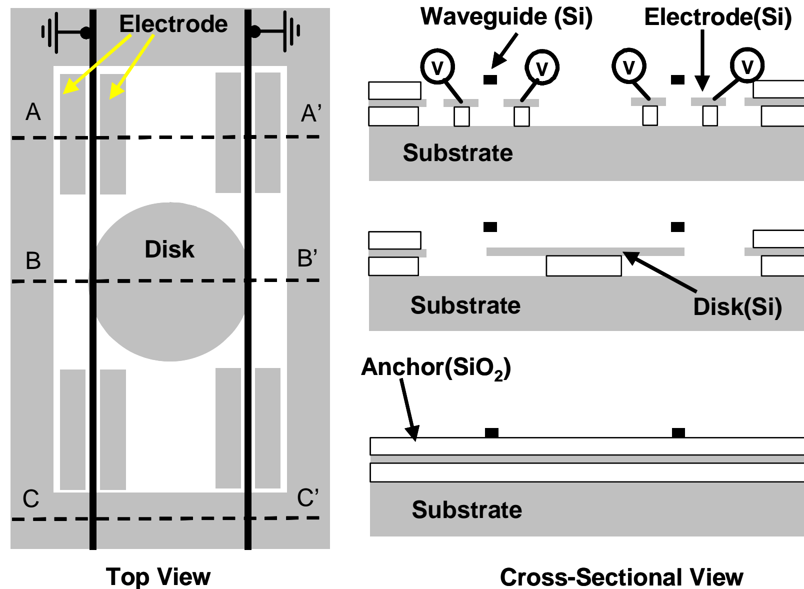

Fig. 1. Schematic illustration of a vertically-coupled microdisk resonator integrated with MEMS actuators. The top view is shown on the left. The right pictures depict the cross-sections at different locations: actuator (AA'), microdisk (BB'), and waveguide anchor (CC'). The waveguides are electrically grounded.

The fabrication process is described as follow. First, a thin silicon dioxide film (200-nm thickness) was deposited on a SOI wafer with 0.25-μm top silicon and 1-μm buried silicon dioxide (BOX). After photolithography, the microdisk and electrode patterns were transferred to the top SiO_2 layer as a hard mask. The silicon layer was then etched by HBr-based reactive ion etching until the BOX was exposed. The patterned silicon disk was immersed in a buffered HF solution to form a SiO_2 pedestal supporting the microdisk. To reduce the sidewall roughness of a microdisk which dominantly induces optical loss, the microdisk was annealed in hydrogen ambient for 2 minutes. Heated hydrogen gas facilitates the surface diffusion of silicon atoms. The details of this process are reported in [12]. Next, another SOI wafer was coated with SiO_2 via thermal oxidation. The thickness of the silicon layer was then decreased to 0.26 μm, while a 1-μm SiO_2 film was grown on top of the silicon after the thermal oxidation. The top surfaces of the oxidized SOI and the patterned SOI were subsequently bonded for one hour in a high temperature (900°C) furnace. The substrate and the BOX layer of the second SOI wafer were removed by mechanical lapping combined with chemical etching process until only the thin silicon film remained on the microdisk, with the coated SiO_2 as a spacer. To accomplish well coupling in our device, the waveguide patterns are precisely aligned to the microdisk through a Nikon stepper. After the waveguides were fabricated by etching the top silicon film, the wafer was coated with a photoresist as a mask for releasing windows. The wafer was further diced into test samples, and each sample was immersed into diluted HF (6:1) to release the waveguides while keep other components on the substrate. Finally, the photoresist was removed with acetone, and the sample was dried in a critical-point drying process. Figure 2 shows the SEM image of the fabricated device. The microdisk and the electrodes are in the bottom layers, and the two waveguides and electrical

#68804 - $15.00 USD Received 8 March 2006; accepted 5 May 2006
(C) 2006 OSA

shields are in the top layers. The disk radius is 20 μm with a thickness of 0.25 μm. The released length of the waveguide is 100 μm long and the waveguide width and thickness were measured to be 0.8 μm and 0.26 μm, respectively. The as-fabricated gap spacing between waveguide and disk is 1 μm.

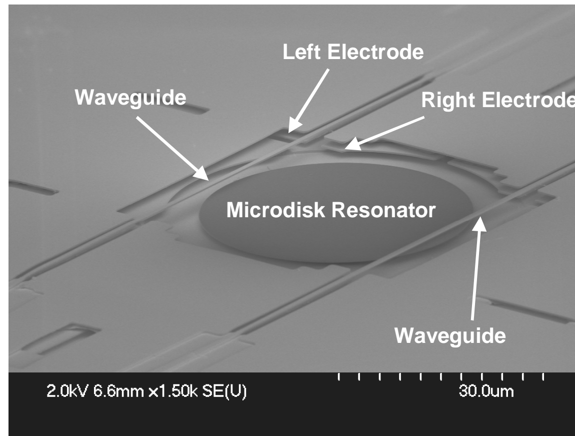

Fig. 2. Scanning electron micrograph of the fabricated device.

3. Analysis and experimental results

3.1. Gap-controlled tunable power coupling ratios

MEMS actuators are utilized for adjusting the gap spacing by deforming the waveguide. Figure 3(a) illustrates the cross-section of the MEMS actuator. The waveguide, shields, and substrate are electrically grounded. As the electrodes are biased, the suspended waveguide is pulled down by the electrostatic force. Thus, the entire waveguide is deformed with the largest displacement at the center position where the disk and the waveguide are efficiently coupled. The electrical shields, as shown in Fig. 3(a), induce a larger net downward force by blocking the electrical fields acting on the top surface of waveguide. Figure 3(b) exhibits the gap variation versus the applied voltage calculated by the commercial simulation tool (ANSYS). The initial gap spacing is 1μm. With electrical shields, the waveguide is apparently actuated with a smaller voltage for a larger displacement. Therefore, the operation range of applied voltage can be reduced (0V ~ 40V) to achieve a complete gap closing.

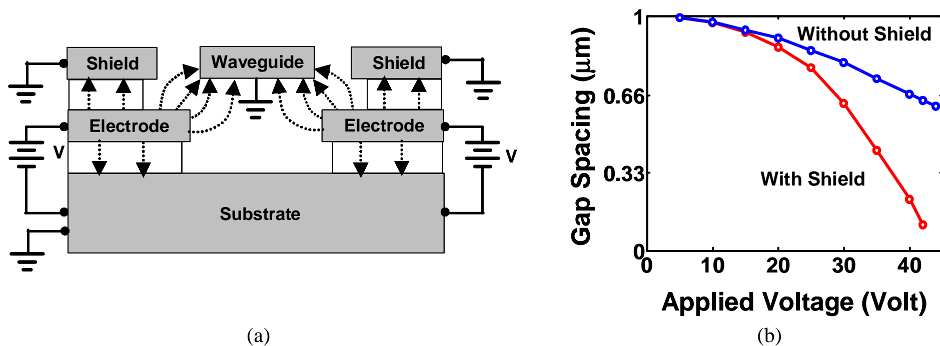

Fig. 3. Mechanical analysis of a MEMS actuator: (a) the cross-section, where dashed arrows represent electrical fields, and (b) simulated curves of the gap spacing as a function of the applied voltage. The two curves are the gap variations with and without electrical shield, respectively.

#68804 - $15.00 USD
Received 8 March 2006; accepted 5 May 2006
(C) 2006 OSA

A power coupling ratio is primarily dependent on the coupling coefficient and the coupling length where the waveguide and the microdisk are well coupled. Figure 4(a) illustrates the schematic of vertical coupling. Since the waveguide is thin, the transverse evanescent fields of guided modes substantially extend along the vertical direction, resulting in a strong coupling with the bottom microdisk. The coupling coefficient is proportional to the overlap integral of electric fields of a waveguide mode and a whispering gallery mode (WGM). Due to the circular profile of a disk, the coupling coefficient actually varies with the vertical gap spacing and each point along the waveguide. At the tangent point, the coupling intensity is maximal and it diminishes as the waveguide deviates from the disk edge. Figure 4(b) displays the analytic coupling coefficient of the device. The horizontal axis represents the deviation from the tangent point. It shows the coupling coefficient is minute as the gap spacing is more than 0.6 μm. Meanwhile, the coupling coefficient is only substantial within a short coupling length, which is estimated to be 10 μm for this device. This coupling length, actually, is proportional to the waveguide width and the radius of the microdisk. To analyze the power coupling ratio, the conventional coupled mode theory for parallel waveguides has to be modified for considering the variable coupling coefficient and nonparallel longitude wavevectors [13]. Figure 4(c) displays the analytic power coupling ratio as a function of gap spacing for a 20-μm-radius silicon microdisk. The waveguide and the disk are assumed with equivalent thickness and phase-match. As the thickness (d) is less than 0.3μm, a 100% power coupling ratio can be achieved.

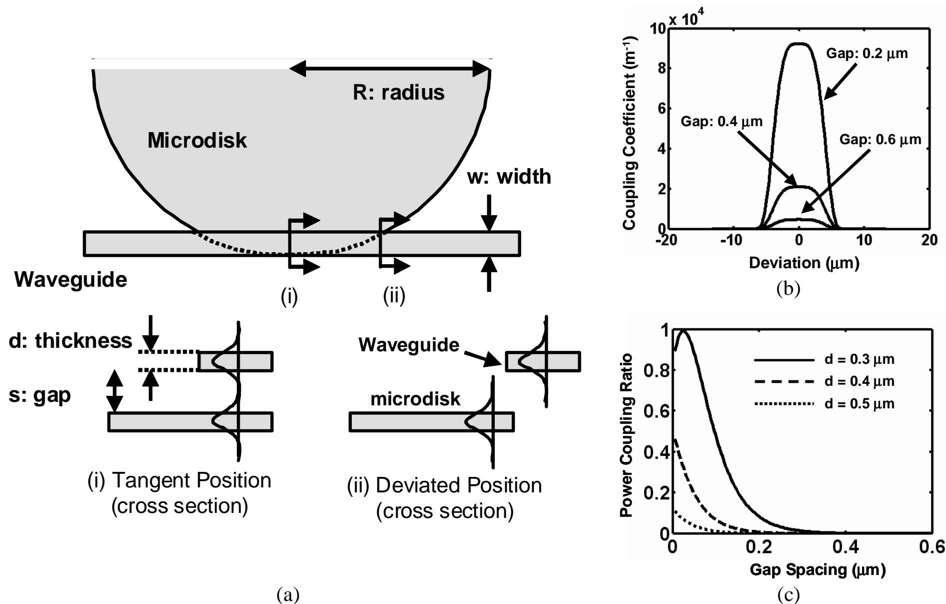

Fig. 4. Analysis of variable power coupling ratios: (a) illustration of vertical coupling, (b) coupling coefficients versus points along the waveguide and gap spacing, and (c) gap-controlled power coupling ratios.

3.2. Experimental results in tunable coupling regimes

The optical transmission of a microdisk-coupled waveguide depends on the resonant frequency, the resonator loss and the power coupling ratio between the waveguide and disk. According to the time-domain coupling theory [14], the optical transfer function of the waveguide is formulated by

#68804 - $15.00 USD Received 8 March 2006; accepted 5 May 2006
(C) 2006 OSA

$$F(\omega) = \frac{j2t_R(\omega - \omega_0) + (\gamma - \kappa)}{j2t_R(\omega - \omega_0) + (\gamma + \kappa)}. \quad (1)$$

where t_R is the round-trip propagation time, ω_0 is the resonant frequency, γ is the round-trip resonator loss, and κ is the power coupling ratio between the waveguide and disk. Among these parameters, ω_0 is determined by the size and the refractive index of the disk. γ is approximately equal to $2\pi R\alpha$ where R is the radius and α is the propagation loss. The propagation loss primarily results from optical absorption and radiation in the material. κ is dramatically dependent on the gap spacing, which is controlled by MEMS actuators in our device. Like microwave resonators, the microdisk can operate in one of the three coupling regimes: under-coupling ($\kappa < \gamma$), critical coupling ($\kappa = \gamma$) and over-coupling ($\kappa > \gamma$). At the resonant frequency ($\omega = \omega_0$), the optical transmission intensity is simply determined by the ratio of resonator loss and the power coupling ratio. It is given by

$$T(\omega_0) = \left|F(\omega_0)\right|^2 = \left(\frac{1-\kappa/\gamma}{1+\kappa/\gamma}\right)^2. \quad (2)$$

The optical transmittance is zero as the microdisk operates in the critical coupling condition. In this case, all the waveguide power is transferred to the microdisk and consumed inside in a form of optical loss. However, the transmittance in the under-coupling and the over-coupling regime ranges from 0 to 1, although the optical phase is actually different by π according to Eq. (2).

In this paper, tunable coupling regimes are demonstrated on a single-waveguide-coupled microdisk, the power coupling ratio of which is controlled by a MEMS actuator deforming the waveguide. The integrated microdisk-waveguide device was characterized in the optical telecommunication band (1,520 nm – 1,565 nm wavelength band). A lensed fiber connected to an amplified-spontaneous-emission (ASE) source was used to launch constant, broad-band wavelengths through the waveguide. Another lensed fiber, aligned to the other facets of the waveguide, collects the output light and is connected to an optical spectrum analyzer (OSA) with a 10-pm resolution to measure the transmission spectra. The measured transmission spectra are shown in Fig. 5. These spectra are centered at the resonant wavelength of 1,549.37 nm. Without bias, the straight waveguide keeps a distance of 1 μm from the microdisk, and inherently no optical power is coupled to the WGM in light of negligible coupling coefficient (Fig. 5(a)). Consequently, all the optical power is transmitted to the output end. As the applied voltage increases, the waveguide is bent toward the microdisk. The power coupling ratio gradually increases until it is equal to the round-trip resonator loss, causing the transmission to drop swiftly at 1,549.37 nm (Fig. 5(b)). The microdisk is operating in the critical coupling condition. The gap spacing further decreases upon increasing the bias, resulting in a larger power coupling ratio than the resonator loss (over-coupling regime), causing the transmission intensity to increase (Fig. 5(c)).

#68804 - $15.00 USD Received 8 March 2006; accepted 5 May 2006
(C) 2006 OSA

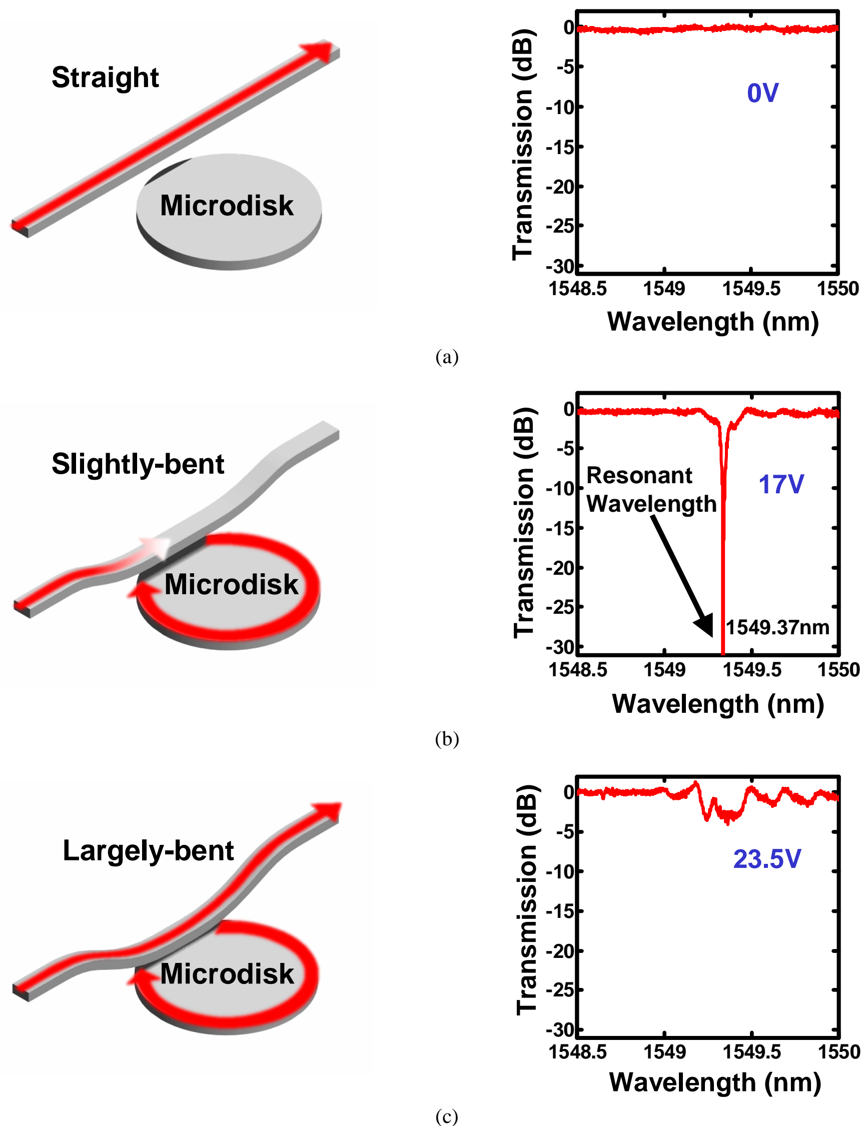

Fig. 5. Transmission spectra for (a) decoupling, (b) critical coupling and (c) over-coupling. The resonant wavelength shown in these spectra is 1549.37nm.

To scrutinize the transition of coupling regimes, the measured optical transmission was plotted as a function of the voltage applied on the actuation electrodes at a resonant wavelength of 1549.37 nm. The result is shown in Fig. 6. The transmission intensity diminishes as the microdisk operates close to the critical coupling condition, occurring at a bias of 17 V. The measured optical transmission is -30dB. The unloaded Q is estimated to be 100,000, which is obtained from analyzing the 3-dB bandwidth of the transmission spectrum in the critical coupling condition. To our knowledge, this is the first time that the various coupling regimes are completely tunable in a semiconductor microdisk resonator device with this gap-controlled mechanism.

#68804 - $15.00 USD
Received 8 March 2006; accepted 5 May 2006
(C) 2006 OSA

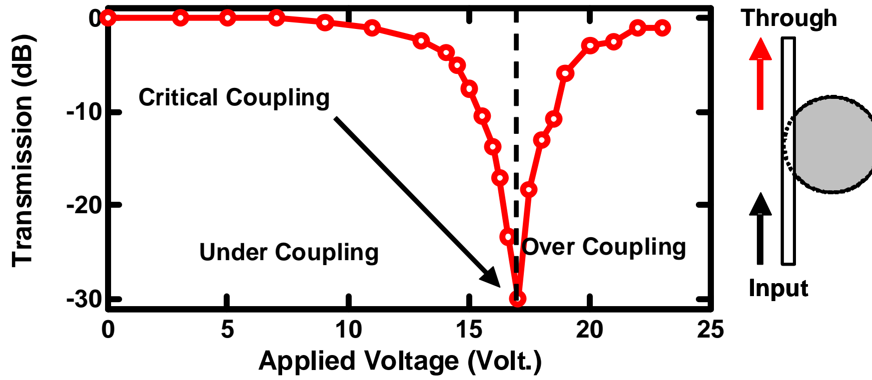

Fig. 6. Transmission curve of a microdisk-coupled waveguide at the resonant wavelength.

3.3. Experimental results in variable chromatic dispersion

In addition to the transmission intensity, the transmission phase of optical waves is also affected by microresonators. The induced phase response, derived from the transfer function in Eq. (1), is given by:

$$\phi(\omega) = \angle F(\omega) = \angle\left[\left(\gamma-\kappa\right)+j2t_R\left(\omega-\omega_0\right)\right]-\angle\left[\left(\gamma+\kappa\right)+j2t_R\left(\omega-\omega_0\right)\right] \tag{3}$$

In this equation, the optical phase varies with the power coupling ratio (κ). The MEMS-actuated microdisk resonator thus enables optical phase engineering by directly controlling the gap spacing. This phase modulation has many applications such as asymmetric MZIs (Mach-Zehnder Interferometers) and tunable array waveguides. Additionally, the first-order derivative of phase response, corresponding to the group delay time, is given by

$$\tau(\omega) = -\frac{d\phi(\omega)}{d\omega}. \tag{4}$$

The group delay time can also be tuned by altering the power coupling ratio through the gap-controlled mechanism. Tunable group delay is useful in dynamically compensating the chromatic dispersion in the optical network or generating optical delay time in optical communication.

Figure 7(a) plots the analytic phase response of the microdisk resonator which operates in the under-coupling and over-coupling regimes. The intrinsic Q of microdisk is assumed to be 100,000, which is associated with a round-trip resonator loss (γ) of 0.02. The detuned frequency is defined as the deviation from the resonant frequency, which is at the center of the spectra. As the microdisk operates in the under-coupling regime, the total phase variation across the entire band is 0. Only when the detuned frequency is close to 0, there is an abrupt phase change with a positive slope. On the contrary, the total phase variation is 2π when the disk operates in the over-coupling regime. The phase changes swiftly with a negative slope at the resonant frequency. The slopes tend to be sharp as the operation of resonator approaches to the critical coupling. Figure 7(b) exhibits the group delay time derived from the phase response. In the under-coupling regime, the group delay turns negative in the vicinity of resonant frequency. On the other hand, the group delay remains positive in the over-coupling regime and tends to decrease with a large power coupling ratio.

#68804 - $15.00 USD
Received 8 March 2006; accepted 5 May 2006
(C) 2006 OSA

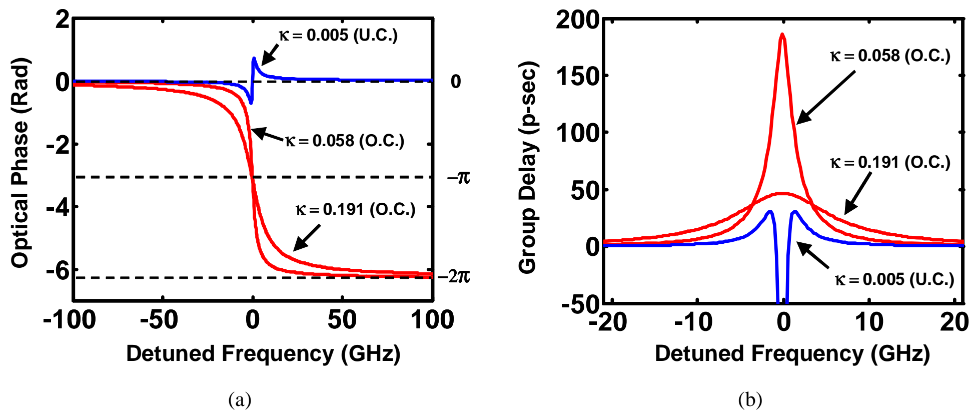

Fig. 7. Analytic chromatic dispersion of (a) optical phase and (b) group delay. The curves represent the operations in the over-coupling (O.C.) and the under-coupling regimes (U.C.).

The group delay is measured with microwave modulation technique. An external cavity tunable laser is employed as the optical source. The optical carrier is modulated by a 500MHz sinusoidal signal. The detected microwave phase shift through the device is monitored while the optical wavelength is tuned across the resonance with a step size of 0.01 nm. The measured phase shift is further transformed into delay time. Figure 8 shows the measured group delay time versus applied voltage. At a bias of 23.7V, a peak group delay of 65 ps is measured (Fig. 8(a)). At a bias of 34.3V, the peak delay is reduced to 27 ps (Fig. 8(c)). A slight shift (0.05 nm) of resonant wavelength is caused by phase mismatch between the microdisk and waveguide due to fabrication variation. The fluctuation of measured data could result from Fabry-Perot etalon at the two ends of the waveguide. By fitting the experimental data to the theoretical curve according to Eq. (4), the power coupling ratios are found to be 0.12, 0.2, and 0.34, at biases of 23.7V, 29V, and 34.3V, respectively. The group velocity dispersion is varied from 185 ps/nm to 1200 ps/nm by taking the maximum positive slopes of the curves.

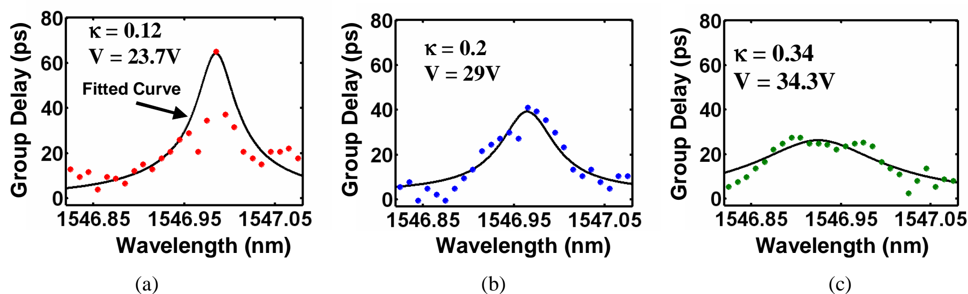

Fig. 8. Measured group delay spectra at various bias voltages: (a) 23.7V, (b) 29V and (c) 34.3V. The power coupling ratios are extracted by fitting the experimental data to the theoretical curves.

6. Conclusion

A vertically-coupled silicon microdisk resonator integrated with MEMS actuators is demonstrated for the first time. The waveguides, MEMS actuators and microdisks are fabricated on a two-layer SOI substrate. Using the MEMS actuation, the waveguide deforms for adjusting the gap spacing between the waveguide and disk, which results in a variable power coupling ratio. Experimental measurement shows the microdisk can dynamically

#68804 - $15.00 USD Received 8 March 2006; accepted 5 May 2006
(C) 2006 OSA

operate in either under-, critical, or over-coupling regime. A high extinction ratio (30dB) and a high quality factor (100,000) are measured in the critical coupling condition. Tunable optical phase and group delay time of propagating wave are also demonstrated by controlling the driving voltage of the MEMS actuators. The microdisk shows the ability to tune the peak group delay from 27 ps to 65 ps and the group velocity dispersion from 185 ps/nm to 1200 ps/nm. This device can be a fundamental building block to construct resonator-based reconfigurable photonic integrated circuits.

Acknowledgments

The work is supported by DARPA through CSWDM program and NSC (Project ID: 95-2221-E-007-002) in Taiwan.